LRP 431/91 August 1991

Papers contributed to the

16th International Conference on Infrared and Millimeter Waves

Lausanne, Switzerland, August 26-30, 1991

CONTENTS

DAPHNE: A programming environment for Gyrotron optimization

R. Gruber, S. Merazzi, T.M. Tran

Centre de Recherches en Physique des Plasmas
Association Euratom-Confédération Suisse
Ecole Polytechnique Fédérale de Lausanne
CH-1007 Lausanne

Abstract:

The user-friendly programming environment DAPHNE has been developed for the optimization of Gyrotrons. It is embedded into the ASTRID system which is an integrated program development system including the module MiniM to define the geometry of the device, the CASE module to describe the boundary conditions, a MESH module to specify an autoadaptive grid, a solver for elliptic partial differential equations, as well as a powerful graphics system. These ASTRID modules are connected together by means of the data management system MEMCOM. External programs (magnetic field solver, particle pusher, wave/beam simulator, heat deposition) can be added by interfacing them to MEMCOM. The different program modules are executed by means of a specially concepted command language. Domain decomposition techniques are used to specify the geometry, to build locally structured meshes and to represent graphically the results.

(1) Gyrotron simulation model

The gyrotron (Fig. 1) we are dealing with consists of a cathode to inject the electron beam, a beam acceleration region (Fig. 2), a region in which the beam is compressed by a magnetic field, a wave/beam interaction region (the cavity, Fig. 3) and an electron beam collector. The model we consider for our simulation is:

(a) The electron gun and the magnetic coils are axisymmetric.

(b) The electric field E is given by $\mathbf{E} = -\nabla\Phi$ and $\Delta\Phi = -\rho/\varepsilon_0$.

(c) The magnetic field is not affected by the electron beam current. It is computed on each mesh point by applying Biot-Savart's law.

(d) The electrons are pushed in the electromagnetic field by solving the relativistic Lorentz equations:

$$\frac{d\mathbf{r}}{dt} = \mathbf{v}, \quad \frac{d}{dt}\gamma\mathbf{v} = \frac{q}{m}(\mathbf{E} + \mathbf{v}\times\mathbf{B}), \qquad \gamma = (1-v^2/c^2)^{-1/2}$$

(2) DAPHNE simulation platform

The DAPHNE gyrotron simulation platform is embedded in the ASTRID programming environment [1]. Three modules of DAPHNE were written specially: The Biot-Savart program CMFI, the particle pusher PART which advances a certain number of specially chosen electrons in the electromagnetic field to enable computing of a precise charge density distribution needed as right hand side vector of the Poisson equation and the electron beam collector module COLL which computes the time-dependent heat transfer. These modules communicate with each others and with the ASTRID modules through the data management system MEMCOM (see Fig. 4). The input for CMFI and PART are given in the input datasets for the ASTRID module CASE. The input datasets for the ASTRID modules are interpreted by a specially concepted command language.The overall DAPHNE architecture is shown in Fig. 4.

The modules are executed in the standard UNIX way, the input datasets interpreted by the command language and data is read from and written back to the data base MEMCOM. The modules are executed in the following order:

MiniM	sets the subdomains defining the geometry of the gun (23 subdomains for our example)
CASE	sets the Dirichlet boundary conditions for the gun
MESH	constructs an initial structured mesh in each subdomain of the gun
SOLVE	solves the Laplace equation to find the potential without a charge density distribution
MiniM	sets the magnetic field coils (6 in our example)
CASE	sets the currents in the coils
CMFI	computes the magnetic field in each mesh point
PART	pushes the electrons and computes the charge density distribution
MESH	reconstructs the mesh using the charge density distribution as mesh density function
CMFI	recomputes the magnetic field in the new mesh points

At this point of the computation we fix the mesh and the magnetic field and iterate over Poisson's equation and the electron trajectories until convergence by executing:

SOLVE	solves the Poisson equation to find the potential
PART	pushes the electrons and computes the charge density distribution

After each of the upper described steps, we can execute
VIEW to represent the results.

If a steady state solution is reached, it is possible to compute the time-evolution of the collector temperature. The time-dependent charge density and velocity distributions on the internal collector wall measure the energy deposition on the surface. The modules to be executed are:
CASE prescribes the time dependent beam characteristics and the cooling conditions
SOLVE solves the time dependent heat transfer equation
VIEW animates the temperature distribution as a function of time.

(3) Results

The DAPHNE program has been applied to compute a practical 100 Ghz gyrotron for fusion plasma heating purposes.Every 102 ms the beam of 2MW power is on for 10 ms. The geometry of the gun is shown in Fig. 1. The potential distribution and the autoadaptive mesh of the beam acceleration region is given in Fig. 2. The electrons are launched at equidistant positions at the surface of the cathode by giving them a normal inflow velocity corresponding to a temperature of 1000°C.Figure 3 shows the potential depression produced by the electron beam in the cavity region. A quantitative comparison of the obtained results with those produced by the EGUN code [2] is shown in Fig. 5. In Figure 6 we present the time evolution of the hottest collector point, the outer surface being cooled at 30°C. For an infinite number of heat sequences, the temperature will reach 180°C.

References:

[1] E. Bonomi, M. Flück, R. Gruber, R. Herbin, S. Merazzi, T. Richner, V. Schmid, C.T. Tran, "ASTRID: A Programming Environment for Scientific Applications on Parallel Vector Computers", *Scientific Computing on Supercomputers II* (Plenum Press, NY, J.T. Devreese and P.E. van Camp, eds., 1990) 51-82
[2] W.B. Herrmannsfeldt, "Electron trajectory program", SLAC Rep. 226, Standford Univ., 1979

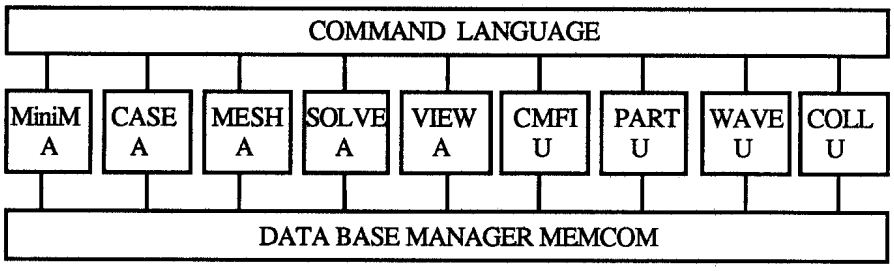

Fig. 4: Software architecture of DAPHNE. The marks A denote modules coming from the ASTRID programming environment, the marks U denote user defined modules.

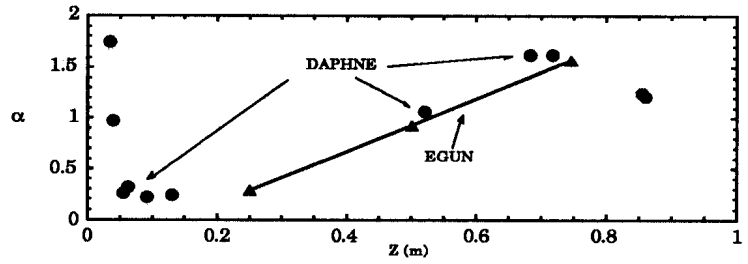

Fig. 5: The electron beam velocity ratio versus the axial coordinate as obtained from the EGUN code and the DAPHNE code.

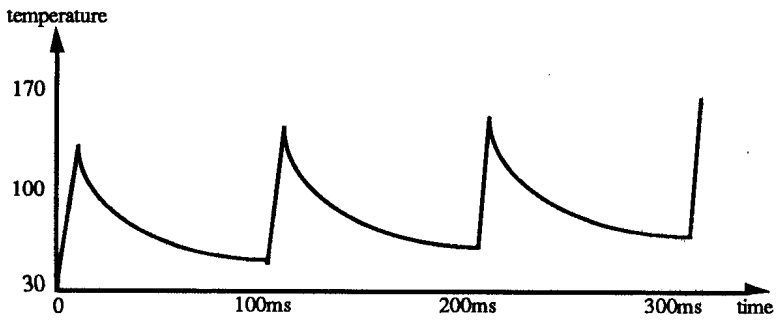

Figure 6: Time evolution of maximum temperature of the beam collector.

Fig. 1 The electron trajectories in a gyrotron, from the gun emitter to the beam collector.

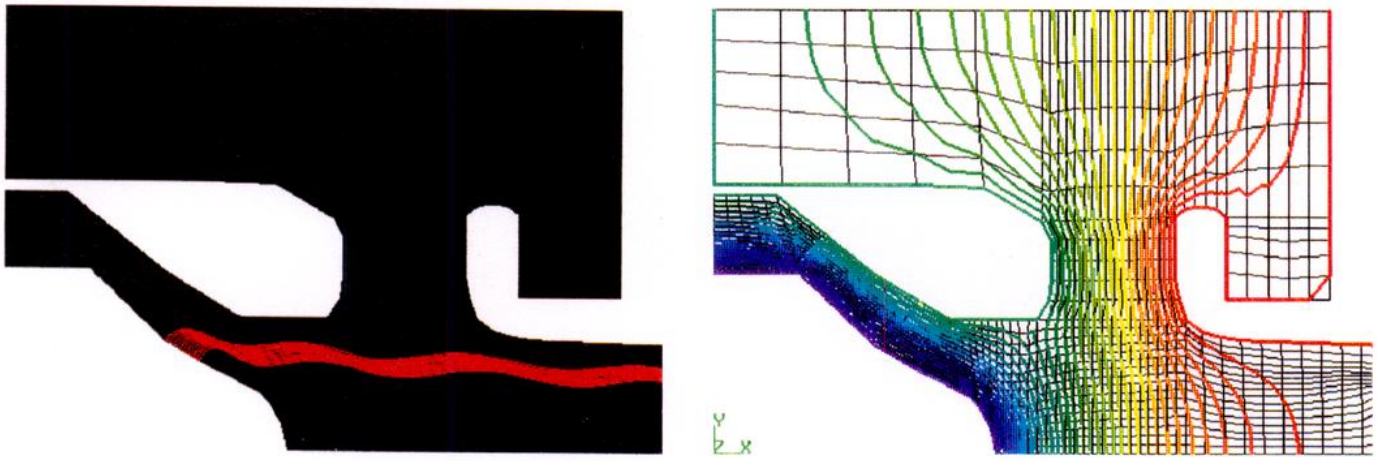

Fig. 2 The electron trajectories and the self-consistent electric potential field at the gun emitter region.

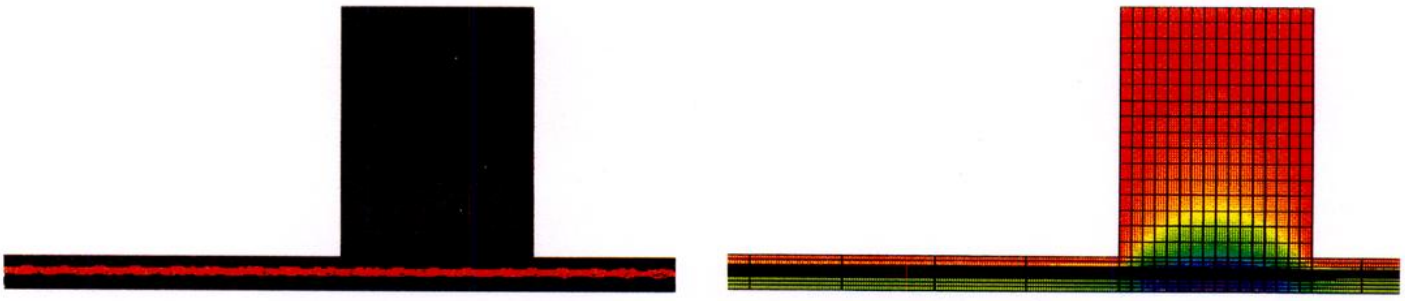

Fig. 3 The electron trajectories and the self-consistent electric potential field at the interaction region.

DETERMINATION OF THE ELECTRON BEAM VELOCITY IN A GYROTRON BY MEANS OF THOMSON SCATTERING

G. Soumagne, M.R. Siegrist, M.Q. Tran

Centre de Recherches en Physique des Plasmas
Association Euratom - Confédération Suisse
Ecole Polytechnique Fédérale de Lausanne, Switzerland

In experimental investigations of gyrotrons an important discrepancy between the theoretically predicted efficiency and measured values has been observed. [1] Since the energy conversion efficiency depends critically on the electron velocity, it is important to be able to measure this latter one. A non-intrusive measurement is only possible with optical methods.

Thomson scattering of laser radiation from electrons has become a standard diagnostic method in plasma physics to measure the electron temperature. We intend to apply this method to determine the relativistic electron velocity in the 100 GHz quasi-optical gyrotron in our laboratory. [1]

The major problem in this experiment is related to the low electron density in the beam (10^{11}-10^{12} cm^{-3}), resulting in a very weak scattered laser signal. It is therefore of paramount importance to optimize the scattering geometry for maximum light collection.

The two variable parameters are the interaction length of the laser beam with the electron beam and the solid angle of the collection optics. The former is maximum for antiparallel light injection (the presence of the cathode does not allow parallel injection), whereas the latter can be optimized by profiting from the cylinder symmetry of the problem. Indeed, light scattered in any direction perpendicular to the common axis of light beam and e-beam contains the same information, except for polarization effects. Hence a cylindrical mirror of parabolic shape can collect scattered light over an angle of 90° or more in one direction and over the interaction length which is only restricted by access. Fig. 1 shows a cut through the interaction region, whereas in Fig. 2 the proposed scattering arrangement is sketched.

The light collection capacity of this system is quite significant, but unfortunately the laser pulse hits directly the cathode of the electron gun. The intensity therefore has to be reduced to a safe level.

The differential scattering k vector in this arrangement forms an angle of 45° with the electron beam direction and hence the spectra should contain information on both the parallel and the perpendicular component of the velocity distribution.

Calculations have shown that the spectra consist of two widely separated peaks at 350nm and 750nm for a ruby laser and at 550 and 1150nm for a Nd:glass laser. In both cases the position of the high-frequency peak contains information on the magnitude of the e-beam velocity and the low-frequency peak on the pitch angle of the electron trajectories. This is illustrated in Fig. 3.

We will discuss the overall performance of the proposed experiment and we will present spectra calculated according to the theory of Zhuravlev et al.[2]

REFERENCES

1 S. Alberti et al., Phys. Fluids B 2(7), 1654 (1990).
2 V.A. Zhuravlev et al., Sov. J. Plasma Phys. 7(3), 292 (1981).

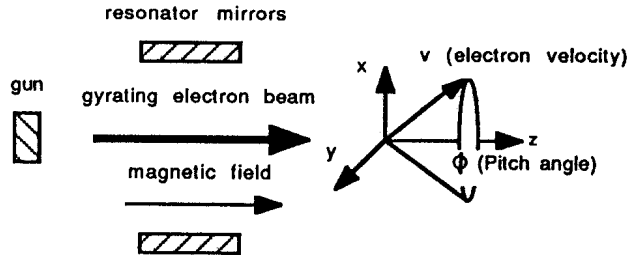

Fig.1. Scheme of quasi-optical resonator.

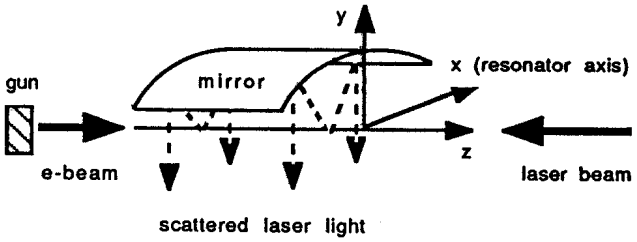

Fig.2. Scheme of scattering geometry.

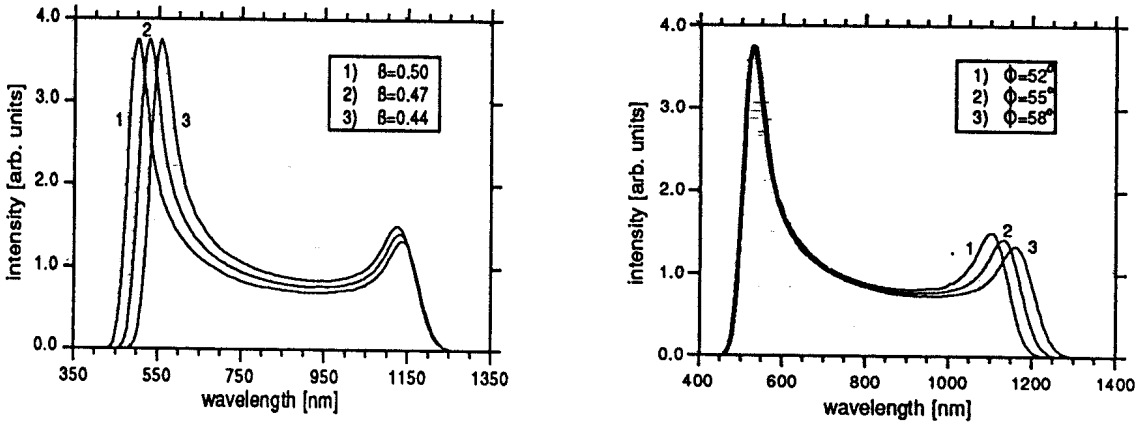

Fig.3. Scattered spectra of gyrating electron beam for Nd:glass laser. Pitch angle fixed at 55°(left), velocity fixed at 0.47 (right).

Experimental study of a quasi optical-gyrotron operating at the second harmonic

S. Alberti and M.Q. Tran
Centre de Recherches en Physique des Plasmas
Association Euratom-Confédération Suisse
Ecole Polytechnique Fédérale de Lausanne
21, Av. des Bains, CH-1007 Lausanne, Switzerland

Abstract

Experimental results of the first operation of a quasi-optical gyrotron on the second harmonic are presented. With a large (mirror separation d = 329mm) unoptimized Fabry-Pérot resonator (ohmic losses = diffractive losses), a nearly monomode emission ($f_{RF} \simeq$ 197GHz) at a power level of 8kW has been measured for a beam current of 3A (V_b = 78kV). Numerical simulations show that operation at the second harmonic is highly sensitive to velocity spread.

Experimental setup

The experimental setup is described in detail in reference [1]. A temperature limited MIG triode electron gun operating at voltages up to 80kV generates an annular electron beam with a mean radius of r_b = 2.26mm in the interaction region. The magnetic field in the interaction region is B_o = 3.98T. Simulations using Hermannsfeldt EGUN code [2] shows that in the gun the ratio $\alpha = v_\perp/v_\parallel$ is a sensitive function of the current I_b, but is always larger than 1.5 for $I_b < 5$A (Fig. 1).

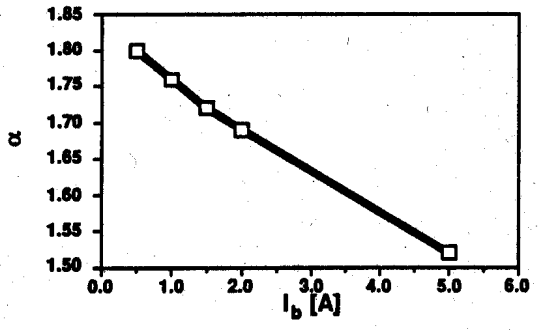

Figure 1: Ratio $\alpha = v_\perp/v_\parallel$ versus beam current I_b ($V_b = 78kV$).

For this experiment, a Fabry-Pérot resonator made of copper, with mirrors of 219mm radius of curvature, a Fresnel number of 1.21 (at 200GHz) and an adjustable separation d of 329mm (±10mm) has been used. The output coupling is purely diffractive [1] and the total quality factors (diffractive + ohmic losses) of the second harmonic and the fundamental are 320000 ($TEM_{0,0,432}$) and 7200 ($TEM_{0,0,217}$), respectively. The ratio ohmic to diffractive losses, L/P, at the second harmonic and the fundamental is $[L/P]_2 = 1.2$ and $[L/P]_1 = 0.01$, respectively.

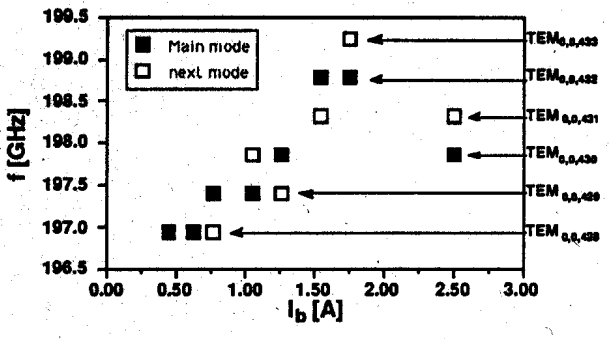

Figure 2: Measured frequency versus beam current.

The radiation waist of the second harmonic is w_{02} = 6.7mm and the spacing between the upstream and downstream beam ducts in the interaction region is 60mm.

For this configuration, the computed minimum starting currents for the second harmonic and the fundamental are I_{stmin2} = 0.7A and I_{stmin1} = 3.6A, respectively.

The diagnostic for the frequency measurement is described in reference [3].

Results and discussion

A minimum starting current of 0.5A has been measured at 196.9GHz ($TEM_{0,0,428}$). The experimentally observed frequency up-shift between the minimum starting current and a beam current of 2A corresponds to 5 longitudinal modes (Fig.2). The longitudinal mode separation is 456MHz. This frequency up-shift is in agreement with a multimode simulation [4] if the current dependent beam depression in the interaction region is taken into account [5].

Within the range of operating current (0–3A) a nearly monomode emission has been observed. A typical spectrum is shown in figure 3.

A continuous frequency tuning has been measured by varying the mirror separation d (Fig. 4). As in the operation at the fundamental [1], a variation of d by half a wavelength leads to a change of the longitudinal mode index by one unit. This behavior is

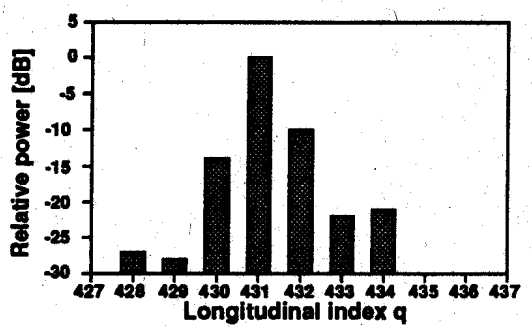

Figure 3: Frequency spectrum measured at a beam current of 2A.

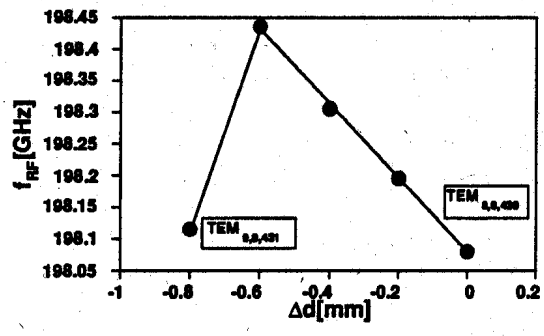

Figure 4: Frequency versus mirror separation d ($\Delta d = 0$ corresponds to $d = 329$mm).

different to the one observed in the case of the parasitic oscillation at the second harmonic reported in reference [3].

The comparison between the measured power versus beam current and the theoretical prediction given by the multimode simulation with no velocity spread is shown in figure 5. The discrepancy between the two curves may be due to the effect of velocity spread. As an example, figure 6 shows the effect of velocity spread on the RF power for a beam current of 2A. This effect is a consequence of the fact that the second harmonic oscillation is a finite Larmor radius effect.

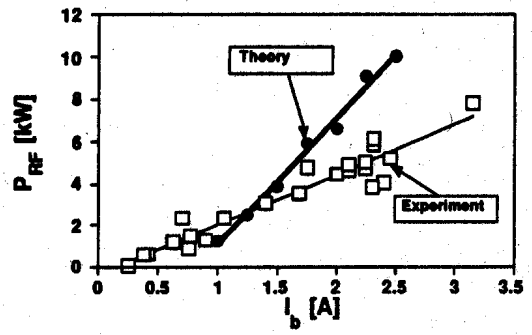

Figure 5: Theoretical and measured RF power versus beam current ($V_b = 78$kV).

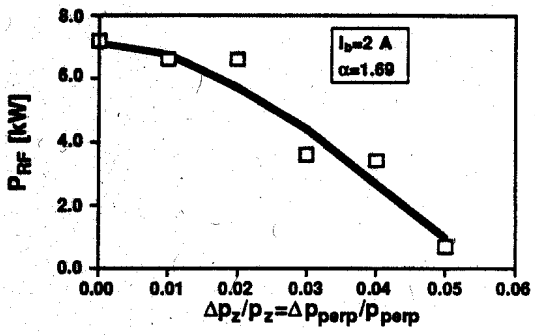

Figure 6: Theoretical RF power versus velocity spread for a beam current of 2A.

Conclusions

The operation of a quasi-optical gyrotron on the second harmonic has been demonstrated. With an unoptimized Fabry-Pérot resonator (diffractive losses = ohmic losses) an RF power of 8kW has been measured at a beam current of 3A (V_b = 78kV). Due to experimental problems, the beam current could not be set at a value higher than the starting current of the fundamental in order to study the competition between the fundamental and the second harmonic. Such a situation has been studied with the multimode code and the simulation shows that the oscillation at the second harmonic is non-linearly suppressed by the fundamental for beam currents $I_b \geq 2I_{stmin1}$, where I_{stmin1} is the minimum starting current of the fundamental.

Aknowledgement

This work was partially supported by the Fonds National Suisse de la Recherche Scientifique under Grant No.20–005652.88.

References

[1] S. Alberti, M.Q. Tran, J.P. Hogge, T.M. Tran, A. Bondeson, P.Muggli, A. Perrenoud, B. Jœdicke, and H.G. Mathews. *Phys. Fluids B*, 2(1654–1661), 1990.

[2] W. Herrmannsfeldt. SLAC Report No.166, Stanford University, Stanford, California, September 1973.

[3] S. Alberti, M.Pedrozzi, M.Q. Tran, J.P. Hogge, T.M. Tran, P. Muggli, B. Jœdicke, and H.G. Mathews. *Phys. Fluids B*, 11(2544–2546), 1990.

[4] T.M. Tran, F. Dufaux, S. Alberti, D. Monselesan, and M.Q. Tran. In R.J. Temkin, editor, *Proc. Fifteenth Int. conference on infrared and millimeter waves, Orlando(Florida), 1990*, pages 209–211, 1990.

[5] S. Alberti, M.Q. Tran, and T.M. Tran. *Phys. Fluids B*, 3(519–521), 1991.

ELLIPSOIDAL DIFFRACTION GRATING AS OUTPUT COUPLER FOR QUASI-OPTICAL GYROTRONS

J.P. Hogge, H.Cao, W.Kasparek*, T.M.Tran, M.Q.Tran, P.J.Paris

Centre de Recherches en Physique des Plasmas
Association Euratom-Confédération Suisse
Ecole Polytechnique Fédérale de Lausanne
21, Av. des Bains, CH-1007 Lausanne, Switzerland

*Institut für Plasmaforschung
Universität Stuttgart, Pfaffenwaldring 31, D-7000 Stuttgart 80, F.R.G.

ABSTRACT

The use of a diffraction grating arranged in the -1 Littrow mount as an output coupler for a quasi-optical Fabry-Pérot resonator at microwave frequencies (100 GHz) was suggested in 1990 [1]. A planar grating with curvilinear grooves (in order to match the Littrow condition everywhere on the surface for a given Gaussian beam) gives a power coupling efficiency of 85%, which is limited by the depolarization induced by the curvature of the grooves. An ellipsoidal grating with linear, equidistant grooves minimized the depolarization but gave approximately the same global efficiency because of distortion. We report low power tests on an improvement of the second scheme, based on curved grooves on an ellipsoidal surface, which gives a global efficiency of 94%.

THE GRATING OUTPUT COUPLER

It has been shown in [1] that power can be efficiently coupled out of a Fabry-Pérot resonator in the millimeter waves range by replacing one of the mirrors of the cavity by a diffraction grating placed in Littrow mount. If d is the groove spacing, θ the angle of incidence, λ the wavelength and n the order of diffraction, this condition can be written:

$$2d \sin\theta = n\lambda .$$

If additionnally $\lambda/d<2/3$, only orders n=-1 and 0 can exist. The order -1 is reflected back in the cavity whereas the 0^{th} order gives the output of the resonator (fig. 1).

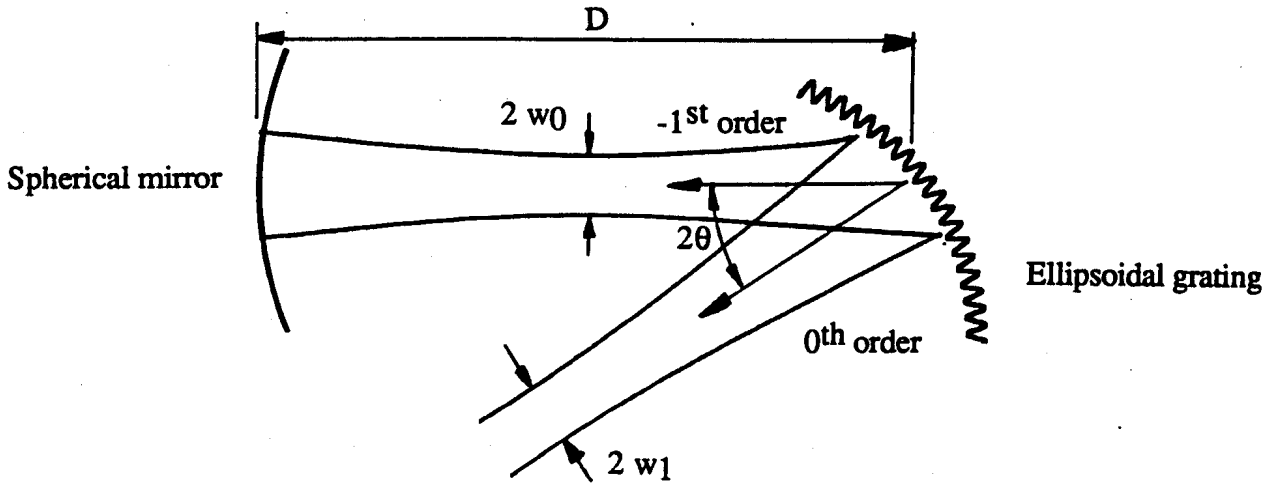

Fig.1: Principle of the grating output coupler.

In order to reproduce the TEM_{00} mode of an equivalent resonator formed by two spherical mirrors, the grooves have to be matched to the phase profile of an incident Gaussian beam of waist w_0, and are thus curvilinear.

In the case of a planar grating, the grooves can be approximated by concentric circles (point source approximation) having their center in the plane of the grating. As the electric field is neither parallel (TE case), nor perpendicular (TM case) to the grooves on almost all the surface of the grating, the amount of induced depolarization is not negligible, typically around 10% [1]. The global efficiency (taking into account the distortion losses, the depolarization losses and the coupling losses to the HE_{11} mode of a corrugated waveguide) is around 85%.

For an ellipsoidal grating, the grooves are much less curved. Such a grating with linear, equidistant grooves gave almost no depolarization, but there was distorsion due to the fact that the Littrow condition was exactly satisfied in the center of the grating only [1]. The global efficiency was comparable to the previous case.

The improvement which was given to the second scheme was to approximate the grooves by circles centered on the axis of revolution of the ellipsoid. A lathe could then be used for the machining and, as the grooves spacing could be modulated, the Littrow condition could be exactly satisfied on one line (perpendicular to the grooves). The experimental results we present here have been obtained with such a grating.

EXPERIMENTAL SET-UP

The microwave power of a carcinotron (f=90-115 GHz, $P_{RF} \leq$ 1W) is coupled into the resonator trough a small hole drilled in the center of the spherical mirror. The quality factor Q of the TEM_{00} modes gives a direct measure of the transparency T, (which is assumed to be equal to the 0^{th} order efficiency) through [2]

$$T=\frac{4\pi D}{\lambda Q},$$

where D is the separation between the spherical mirror and the grating.

The output pattern is recorded by a standard rectangular horn and a Schottky diode mounted on an computer-controlled XY table allowing scans over a 10x10 cm area. The Gaussian content in power c^2 is computed by projecting the measured output pattern E(x,y) of the electric field on the ideal Gaussian distribution

$$c^2=\frac{[\int_S dS\, E(x,y) \exp\{-\frac{(x^2+y^2)}{w_1^2}\}]^2}{[\int_S dS\, E^2(x,y)][\int_S dS \exp\{-\frac{2(x^2+y^2)}{w_1^2}\}]},$$

where w_1 is the waist giving optimum coupling efficiency to the HE_{11} mode of a corrugated waveguide [3]. The cross-polarization content is recorded by rotating the receiving horn by 90°. The parameters of the resonator are : f=92.4 GHz, D=400 mm, kw_0=18, g=-0.7, kw_1=39.47, θ=28 deg, where k is the wavenumber and θ the angle of incidence at the center of the grating. The efficiency in the 0^{th} order is T=10%, computed through the electromagnetic theory of gratings [2]. The grating profile is sinusoidal in order to be compatible with high power applications.These parameters are relevant to the quasi-optical gyrotron operation.

RESULTS

The figure 2 shows the output pattern of the grating resonator for a TEM_{00} mode at 92.4 GHz, measured at the focal point. The lines of equal intensity are separated by 2 dB. The corresponding Gaussian content c^2 is 98.6%. The -8.68 dB line gives a waist kw_1=39.67, which is very close to the ideal value kw_1=39.47. The cross-polarized pattern is shown in figure 3, where the lines are separated by 1 dB. The amount of depolarized signal is 2.9%. Taking into account the fact that a gaussian beam of the right diameter can be coupled to the HE_{11} mode of a corrugated waveguide with an efficiency of 98% [3], the global coupling factor can be estimated to be 94%.

CONCLUSION

We have shown that the use of an ellipsoidal diffraction grating placed in Littrow mount as output coupler for a Fabry-Pérot resonator can lead to a power coupling efficiency of 94%, limited by depolarization losses and coupling to an HE11 waveguide. This type of coupling is going to be implemented on the quasi-optical gyrotron of the CRPP.

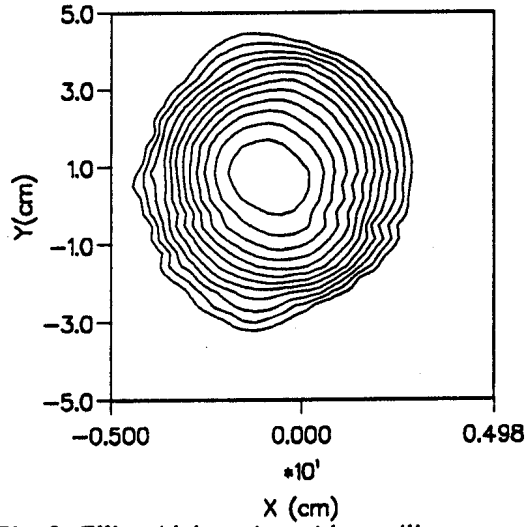

Fig. 2: Ellipsoidal grating with curvilinear grooves: Pattern of a TEM_{00} mode measured at the focal point. Contours of equal intensity are separated by 2dB. The area is 10x10cm.

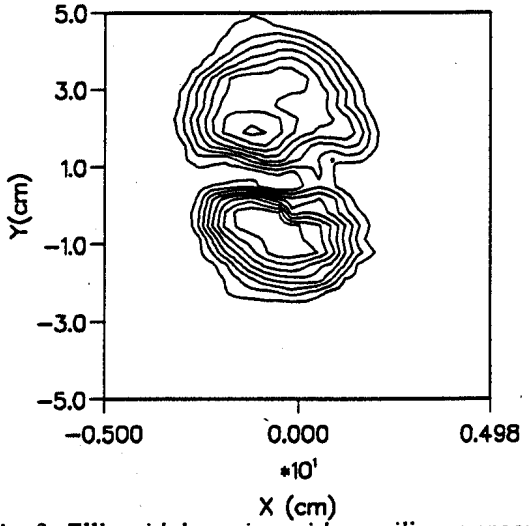

Fig. 3: Ellipsoidal grating with curvilinear grooves: Cross polarization pattern of the mode of fig. 2. Contours are separated by 1dB. The depolarized power content is 2.9%

We would like to acknowledge Mr. Vallon from Les Ateliers Mécaniques de Vevey for the realization of the grating.

[1] J.P.Hogge, H.Cao, W.Kasparek, T.M.Tran, M.Q.Tran, Proc. 15th Int. Conf on Infrared and millimeter Waves, Orlando, Florida, 1990, SPIE 1514, 535 (1990)

[2] See for example: Electromagnetic Theory of Grating, R. Petit, Ed. (Springer Verlag, 1980).

[3] R.L. Abrams, IEEE Trans. Quant. El., QE-8,838, (1972).

DISTORTION AND CROSS POLARIZATION OF A SIMPLE GAUSSIAN BEAM ON DIFFRACTION FROM GRATING COUPLERS FOR Q. O. GYROTRONS

H.Cao, J.P.Hogge, T.M.Tran, M.Q.Tran

Centre de Recherches en Physique des Plasmas, Association Euratom-Confédération Suisse
Ecole Polytechnique Fédérale de Lausanne
21, Av. des Bains, CH-1007 Lausanne, Switzerland

ABSTRACT

We examine the distortion and cross polarization of a Gaussian beam diffracted from a planar grating with curvilinear grooves or from an elliptical grating with curved grooves placed in the Littrow mount. The electromagnetic field diffracted from the gratings in the 0th order and propagating to an HE_{11} waveguide has been numerically computed. The output patterns, distortion, and cross polarization have been obtained for the gratings; the results agree well with the cold test results. The comparison between the gratings shows that the elliptical grating is more effective than the planar grating.

1. INTRODUCTION

Grating coupler systems provide an alternative to mirror edge-coupling in quasi optical (Q. O.) gyrotrons[1,2]. As verified in many cold tests, this method produces an almost perfect Gaussian output pattern. However, the grating coupler we have proposed should meet the Littrow-mount condition at every point on the grating, therefor the grooves are curvilinear and the grating must be off axis. As a consequence the diffracted beam suffers from cross polarization and distortion effects on the field profiles.

For the design of a grating coupler system, the knowledge of the distortion and the cross polarization of a simple Gaussian beam diffracted in 0th order is important in order to determine the type and parameters of the grating for an efficient output coupling in Q. O. gyrotrons. In this paper these effects are quantified for a planar grating with curvilinear grooves and an elliptical grating with curved grooves. Theoretical considerations are based mainly on the electromagnetic theory of gratings[3] and Kirchhoff's diffraction theory[4], taking account of vectorial $\overline{E}$ and $\overline{H}$ fields.

2. PLANAR GRATING WITH CURVILINEAR GROOVES

It is well known from the electromagnetic theory of gratings that the complex diffraction efficiencies in 0th order for the TM and the TE cases are different[3]. The incident $\overline{E}$ field ($\overline{H}$ field) can be decomposed into TM and TE components, taking account of the circular concentric groove shape. The wave diffracted in the 0th order is generated by the incident TM and TE components with the corresponding complex diffraction efficiences in the 0th order R_{tm} and R_{te}. For the calculation of the propagation from the grating to the HE_{11} waveguide, the vectorial diffraction formulae are derived based on Kirchhoff's diffraction theory[4]. An estimate of the Gaussian content in power is found using the method described in [1,2].

3. ELLIPTICAL GRATING WITH CURVED GROOVES

Because the wavefront of a Gaussian beam is parabolic, an elliptical surface will match it better than a plane. The grooves of the elliptical grating are only slightly curved and the groove spacing is rather uniform compared to the planar grating[1,2]. It is expected that distortion and cross polarization should be less than that of planar grating. The output from an elliptical grating coupler system is focused, and can be directly matched to the HE_{11} waveguide. The same principle discussed above for the planar grating was used in the computation.

4. RESULTS AND DISCUSSION

A code was written to solve the integral equations for the planar grating and the elliptical grating. From the theoretical results we can see that the main power is concentrated in the original polarization and that only a few percent of the total energy is in the cross polarization. The output pattern in the original polarization is almost perfectly Gaussian: less than 1% distortion was found for both cases. The output patterns in the cross polarization are high-order modes (Fig. 1, Fig. 2). These results also agree well with the cold test results[5]. The distortion for both gratings is negligible; however, a significant amount of energy is lost in the cross polarization. The energy loss in the cross polarization depends on the curvature of the grooves and the difference between the diffraction efficiences R_{tm}, R_{te} in TM and TE. Because the groove shape of a planar grating is much more curved than the one of an elliptical grating, it should be less for the latter than for the former. In the computation we found that the larger difference between R_{tm} and R_{te} is, the more energy loss is caused by the cross polarization. In the design of a grating, R_{tm} and R_{te} should be selected as close as possible. Cold tests with both gratings have been performed[5] and agreement between computation and cold test results is quite good (shown in table 1) especially in the case of the elliptical grating. We conclude that the

elliptical grating is more effective than the planar grating as an output coupler for Q.O. gyrotrons. The output pattern is almost perfect Gaussian and only few percent energy loss has been found in distortion and cross polarization.

REFERENCES

[1] J.P. Hogge, H. Cao, W. Kasparek, T.M. Tran , M.Q. Tran, Proc. 15th Int. Conf. on Infrared and Millimeter Waves, Orlando, Florida, USA, (1990)

[2] H. Cao, J.P. Hogge, W. Kasparek, T.M. Tran, M.Q. Tran, to be published

[3] See for example: Electromagnetic Theory of Gratings, R. Petit, Ed. (Springer Verlag, 1980)

[4] M. Born and E. Wolf, Principles of Optics, 6th Ed., New York: Pergamon, (1980)

[5] J.P. Hogge, H. Cao, W. Kasparek, T.M. Tran, M.Q. Tran, P.J. Paris, Proc. 16th Int. Conf. on Infrared and Millimeter Waves, Lausanne, Switzerland, (1991)

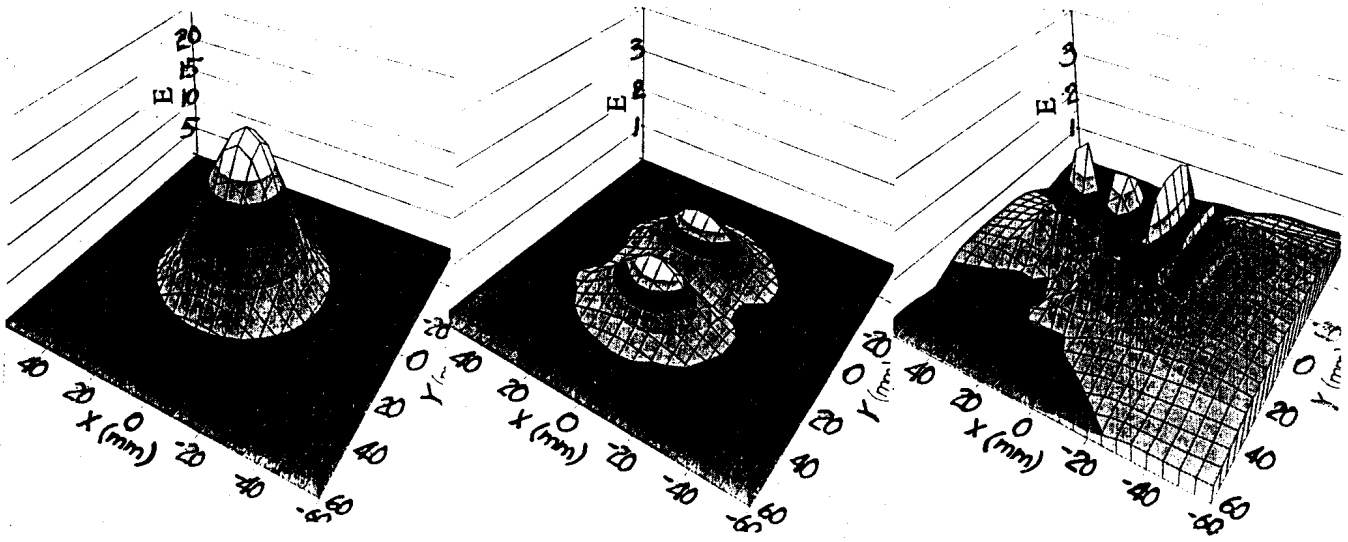

(a) (b) (c)

Fig. 1 Computed output patterns of the electric fields for the planar grating. The grating is used in a Q. O. gyrotron resonator with mirror separation d=216mm and g=-0.55 (a) x; (b) y; (c) z-components

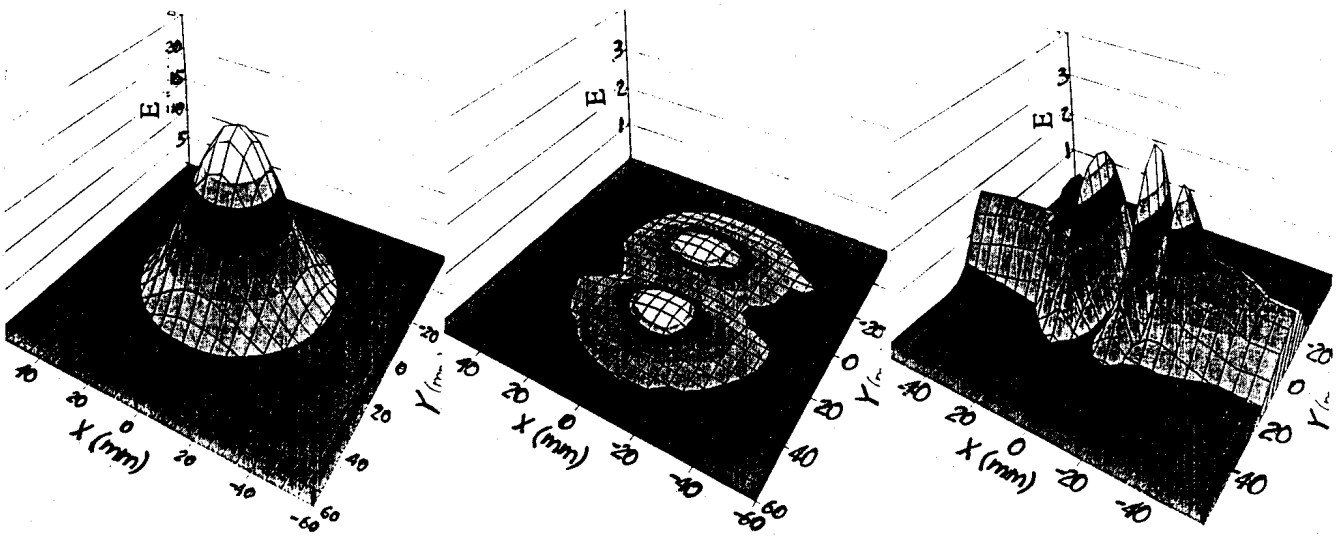

(a) (b) (c)

Fig. 2 Computed output patterns of the electric fields for the elliptical grating, d=400mm and g=-0.7. (a) x; (b) y; (c) z-components

Table 1 Computed distortion and cross polarization compared with cold test results for the resonator described on the figure caption.

	planar grating		elliptical grating	
	computation	cold test	computation	cold test
distortion	<1%	10%	<1%	<1%
cross polarization	4%	7%	2.2%	3%
total	<5%	17%	<3.2%	<4%